(42) suggest that preindustrial levels were <1.9 ppt. Assuming a steady state and a 4.9-year lifetime, these levels imply natural emissions of <10 Gg year^{-1}.
41. J. H. Butler *et al.*, *Nature* **399**, 749 (1999).
42. P. J. Fraser, unpublished data.
43. We estimate emissions of ~1 Gg year^{-1} in Europe in 1999, 0.06 Gg year^{-1} in Australia in 1998–99, and <1 Gg year^{-1} in the western United States in 1999 (*5*).
44. S. Karlsdottir, I. S. A. Isaksen, *Geophys. Res. Lett.* **27**, 93 (2000).
45. M. Mayer, C. Wang, M. Webster, R. Prinn, *J. Geophys. Res.* **105**, 22869 (2000).
46. A. M. Thompson, *Science* **256**, 1157 (1992).
47. Y. Wang, D. Jacob, *J. Geophys. Res.* **103**, 31123 (1998).
48. P. J. Crutzen, P. H. Zimmerman, *Tellus* **43AB**, 136 (1991).
49. The ALE, GAGE, and AGAGE projects involved substantial efforts by many people beyond the authors of this paper (*5*). In its latest phase (AGAGE), support came (and comes) primarily from NASA, with important contributions from the Department of Environment, Transport and the Regions (United Kingdom); Commonwealth Scientific and Industrial Research Organization (Australia); Bureau of Meteorology (Australia); and NOAA, among others (*5*).

28 December 2000; accepted 17 April 2001
Published online 3 May 2001;
10.1126/science.1058673
Include this information when citing this paper.

REPORTS

New Ages for the Last Australian Megafauna: Continent-Wide Extinction About 46,000 Years Ago

Richard G. Roberts,[1]* Timothy F. Flannery,[2] Linda K. Ayliffe,[3]† Hiroyuki Yoshida,[1] Jon M. Olley,[4] Gavin J. Prideaux,[5] Geoff M. Laslett,[6] Alexander Baynes,[7] M. A. Smith,[8] Rhys Jones,[9] Barton L. Smith[10]

All Australian land mammals, reptiles, and birds weighing more than 100 kilograms, and six of the seven genera with a body mass of 45 to 100 kilograms, perished in the late Quaternary. The timing and causes of these extinctions remain uncertain. We report burial ages for megafauna from 28 sites and infer extinction across the continent around 46,400 years ago (95% confidence interval, 51,200 to 39,800 years ago). Our results rule out extreme aridity at the Last Glacial Maximum as the cause of extinction, but not other climatic impacts; a "blitzkrieg" model of human-induced extinction; or an extended period of anthropogenic ecosystem disruption.

Twenty-three of the 24 genera of Australian land animals weighing more than 45 kg (which, along with a few smaller species, constituted the "megafauna") were extinct by the late Quaternary (*1–3*). The timing and causes of this environmental catastrophe have been debated for more than a century (*4, 5*), with megafaunal extirpation being attributed to the impact of the first human colonizers (*1, 5–8*), who arrived 56 ± 4 thousand years ago (ka) (*9–13*), or climate change (*4*) [in particular, increased aridity at the Last Glacial Maximum (19 to 23 ka) (*14*)]. A resolution to this debate has been thwarted by the lack of reliable ages for megafaunal remains and for the deposits containing these fossils. The disappearance of one species of giant bird (*Genyornis newtoni*) from the arid and semi-arid regions of southeastern Australia has been dated to 50 ± 5 ka, on the basis of >700 samples of eggshell (*8*), but no secure ages for extinction have been reported for the giant marsupials or reptiles, which constitute 22 of the 23 extinct genera of megafauna weighing >45 kg. Here we present burial ages, obtained using optical and $^{230}Th/^{234}U$ dating methods, for the remains of several megafaunal taxa (mostly giant marsupials; see Table 1) discovered at sites located in the humid coastal fringe and drier continental interior of Australia and in the montane forest of West Papua (Fig. 1), which was joined to Australia by a land bridge at times of lowered global sea level.

Most major biogeographic and climatic regions, and all five main groups of fossil sites (*14*), are represented in our survey. Most of the sites in southwestern Australia are caves that have acted as pitfall traps,

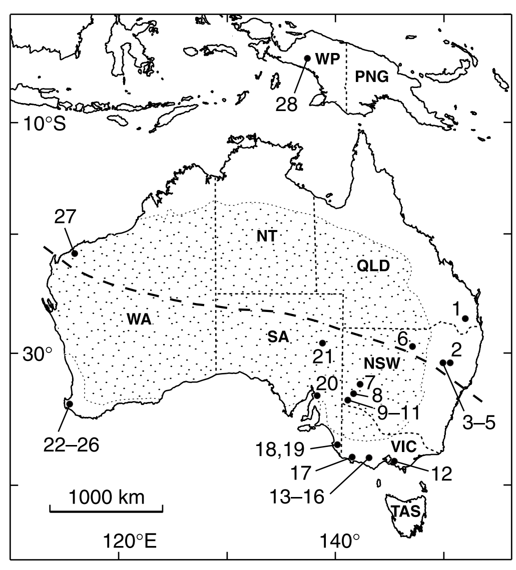

Fig. 1. Map of the Australian region showing the megafauna sites dated in this study. Site numbers: 1, Ned's Gully; 2, Mooki River; 3, Cox's Creek (Bando); 4, Cox's Creek (Kenloi); 5, Tambar Springs; 6, Cuddie Springs; 7, Lake Menindee (Sunset Strip); 8, Willow Point; 9, Lake Victoria (site 50); 10, Lake Victoria (site 51); 11, Lake Victoria (site 73); 12, Montford's Beach; 13, Lake Weering; 14, Lake Corangamite; 15, Lake Weeranganuk; 16, Lake Colongulac; 17, Warrnambool; 18, Victoria Fossil Cave (Grant Hall); 19, Victoria Fossil Cave (Fossil Chamber); 20, Wood Point; 21, Lake Callabonna; 22, Devil's Lair; 23, Kudjal Yolgah Cave; 24, Mammoth Cave; 25, Moondyne Cave; 26, Tight Entrance Cave; 27, Du Boulay Creek; 28, Kelangurr Cave. The bold dashed line crossing the continent indicates the approximate present-day boundary between the zones dominated by summer rainfall from monsoonal activity (north of the line) and winter rainfall from westerly storm tracks (south of the line). The stippled area indicates the zone that receives less than 500 mm rainfall per year and where potential evapotranspiration exceeds mean monthly evapotranspiration year-round with negligible runoff. Climatic data are from (*24, 38*) and references therein.

[1]School of Earth Sciences, University of Melbourne, Melbourne, Victoria 3010, Australia. [2]South Australian Museum, Adelaide, South Australia 5000, Australia. [3]Laboratoire des Sciences du Climat et de l'Environnement, 91198 Gif-sur-Yvette, France. [4]Commonwealth Scientific and Industrial Research Organization (CSIRO) Land and Water, Canberra, ACT 2601, Australia. [5]Department of Earth Sciences, University of California, Riverside, CA 92521, USA. [6]CSIRO Mathematical and Information Sciences, Melbourne, Victoria 3168, Australia. [7]Western Australian Museum, Perth, Western Australia 6000, Australia. [8]National Museum of Australia, Canberra, ACT 2601, Australia. [9]Department of Archaeology and Natural History, Research School of Pacific and Asian Studies, Australian National University, Canberra, ACT 0200, Australia. [10]Department of Earth Sciences, La Trobe University, Melbourne, Victoria 3086, Australia.

*To whom correspondence should be addressed. E-mail: rgrobe@unimelb.edu.au
†Present address: Department of Geology and Geophysics, University of Utah, Salt Lake City, UT 84112, USA.

Table 1. Megafaunal taxa represented at the study sites. The names of the numbered sites are given in Table 2 and Fig. 1. Taxa represented by articulated remains are indicated by **X** and **Cf.**, whereas x and cf. denote taxa represented by disarticulated remains or remains for which articulation is uncertain. Parentheses indicate that *Genyornis newtoni* is represented by a footprint at Warrnambool (site 17) and by eggshell at Wood Point (site 20). The extant *Macropus giganteus*, *M. fuliginosus*, and *Sarcophilus harrisii* are included as they are represented by individuals up to 30% larger in dental dimensions than the living forms. The gigantic form of *M. giganteus* is referred to here as *M. g. titan*, and that of *S. harrisii* as *S. h. laniarius*. *Vombatus hacketti* and *Wallabia kitcheneri* belong to genera extant in eastern Australia but extinct in Western Australia.

Taxa	Site																													
	1	2	3	4	5	6*	6†	7	8	9, 10	11	12	13	14	15	16	17	18	19	20	21	22	23	24	25	26J	26H	26D	27	28
Articulated remains represented	**X**	.	**X**	**X**	.	.	.	**X**	**X**	**X**	**X**	**X**	**X**	.	**X**	**X**	**X**	.	**X**	.	**X**	.	**X**	**X**	**X**	.	.	.	**X**	.
Reptiles																														
Meiolania sp. indet.	.	.	.	.	.	.	x	.	.	.	.	.	.	.	.	.	.	.	.	.	.	.	.	.	.	.	.	.	.	.
Megalania prisca	.	.	.	.	.	.	x	.	.	.	.	.	.	.	.	.	.	.	.	.	.	.	.	.	.	.	.	.	.	.
Wonambi naracoortensis	.	.	.	.	.	.	.	.	.	.	.	.	.	.	.	.	.	.	.	.	.	.	.	x	.	.	.	.	.	.
Pallimnarchus sp. indet.	.	.	.	.		x	x	.	.	.	.	.	.	.	.	.	.	.	.	.	.	.	.	.	.	.	.	.	.	.
Quinkana sp. indet.	.	.	.	.	.	.	x	.	.	.	.	.	.	.	.	.	.	.	.	.	.	.	.	.	.	.	.	.	.	.
Birds																														
Genyornis newtoni	.	.	.	.	.	x	x	.	.	.	.	.	.	.	.	.	(**X**)	.	.	(x)	**X**	.	.	.	.	.	.	.	.	.
Progura naracoortensis	.	.	.	.	.	.	.	.	.	.	.	.	.	.	.	.	.	.	x	.	.	.	.	.	.	.	.	.	.	.
Mammals																														
Megalibgwilia ramsayi	.	.	.	.	.	.	.	.	.	.	.	.	.	.	.	.	.	.	x	.	.	.	.	x	x	.	.	.	.	.
"*Zaglossus*" *hacketti*	.	.	.	.	.	.	.	.	.	.	.	.	.	.	.	.	.	.	.	.	.	.	.	x	.	.	.	.	.	.
Sarcophilus harrisii laniarius	x	.	.	.	.	.	.	.	.	.	x	.	.	x	.	x	.	.	x	.	.	.	.	.	.	.	.	x	.	.
Diprotodon optatum	**X**	x	**X**	**X**	.	x	x	.	.	x	.	.	.	.	.	x	.	.	.	.	**X**	.	.	.	.	.	.	.	**X**	.
Diprotodon sp. indet.	.	.	.	.	x	.	.	.	.	.	.	.	.	x	.	.	.	.	x	.	.	.	.	.	.	.	.	.	.	.
Maokopia ronaldi	.	.	.	.	.	.	.	.	.	.	.	.	.	.	.	.	.	.	.	.	.	.	.	.	.	.	.	.	.	x
Zygomaturus trilobus	.	.	.	.	.	.	.	.	.	.	.	.	.	.	.	.	.	x	**X**	.	.	.	.	**X**	**X**	.	.	x	.	.
Zygomaturus sp. indet.	.	.	.	.	.	.	.	.	.	.	.	.	.	.	.	x	.	.	.	.	.	.	.	.	.	.	.	.	.	.
Palorchestes azael	.	x	.	.	.	.	x	.	.	.	.	.	.	.	.	.	.	.	x	.	.	.	.	.	.	.	.	.	.	.
Phascolonus gigas	x	x	.	.	.	.	x	.	.	**X**	**X**	.	.	x	**X**	.	.	.	.	.	**X**	.	.	.	.	.	.	.	.	.
Vombatus hacketti	.	.	.	.	.	.	.	.	.	.	.	.	.	.	.	.	.	.	.	.	.	x	x	x	.	.	.	x	.	.
Thylacoleo carnifex	x	x	.	.	.	.	.	.	.	x	.	.	.	x	.	x	.	x	**X**	.	.	x	.	x	.	.	.	.	.	.
Propleopus oscillans	.	.	.	.	.	.	.	.	.	.	.	.	.	.	.	.	.	.	x	.	.	.	.	.	.	.	.	.	.	.
Borungaboodie hatcheri	.	.	.	.	.	.	.	.	.	.	.	.	.	.	.	.	.	.	.	.	.	.	.	.	.	.	.	x	.	.
Macropus ferragus	.	.	.	.	.	.	.	.	.	**X**	.	.	.	.	.	.	.	.	.	.	.	.	.	.	.	.	.	.	.	.
Macropus fuliginosus	.	.	.	.	.	.	.	.	.	.	.	.	.	.	.	.	.	.	.	.	.	x	x	**X**	**X**	x	.	.	.	.
Macropus giganteus titan	**X**	x	.	.	.	x	x	.	.	.	x	.	**X**	x	**X**	**X**	.	.	x	.	**X**	.	.	.	.	.	.	.	.	.
Macropus sp. indet.	.	.	.	.	x	.	.	.	.	.	.	.	.	.	.	.	.	x	x	.	.	.	.	.	.	.	.	.	.	.
Procoptodon goliah	x	.	.	.	.	.	.	**X**	.	**X**	x	.	.	.	.	.	.	.	**X**	.	.	.	.	.	.	.	.	.	.	.
Procoptodon sp. indet.	.	.	.	.	x	.	.	.	.	.	.	.	.	.	.	x	.	.	.	.	.	.	.	.	.	.	.	.	.	.
Protemnodon anak	.	.	.	.	.	.	.	.	.	x	.	.	.	.	**X**	x	.	.	.	.	.	.	.	.	.	.	.	.	.	.
Protemnodon brehus	.	.	.	.	.	.	.	.	.	**X**	.	**Cf.**	.	.	.	cf.	.	.	.	.	**Cf.**	.	.	x	.	.	.	x	.	.
Protemnodon hopei	.	.	.	.	.	.	.	.	.	.	.	.	.	.	.	.	.	.	.	.	.	.	.	.	.	.	.	.	.	x
Protemnodon roechus	**X**	.	.	.	.	.	.	.	.	.	.	.	.	.	.	.	.	.	x	.	.	.	.	.	.	.	.	.	.	.
Protemnodon sp. indet.	.	x	.	.	.	.	x	.	**X**	.	.	.	.	.	.	.	.	.	.	.	.	x	.	.	.	.	.	.	.	.
Simosthenurus baileyi	.	.	.	.	.	.	.	.	.	.	.	.	.	.	.	.	.	.	x	.	.	.	.	.	.	.	.	.	.	.
Simosthenurus brownei	.	.	.	.	.	.	.	.	.	.	.	.	.	.	.	.	.	.	**X**	.	.	.	**X**	**X**	**X**	.	.	x	.	.
Simosthenurus gilli	.	.	.	.	.	.	.	.	.	.	.	.	.	.	.	.	.	x	**X**	.	.	.	.	.	.	.	.	.	.	.
Simosthenurus maddocki	.	.	.	.	.	.	.	.	.	.	.	.	.	.	.	.	.	.	x	.	.	.	.	.	.	.	.	.	.	.
Simosthenurus newtonae	.	.	.	.	.	.	.	.	.	.	.	.	.	.	.	.	.	x	x	.	.	.	.	.	.	.	.	x	.	.
Simosthenurus occidentalis	.	.	.	.	.	.	.	.	.	.	.	.	.	.	.	.	.	.	**X**	.	.	.	x	x	.	x	x	x	.	.
Simosthenurus pales	.	.	.	.	.	.	.	.	.	.	.	.	.	.	.	.	.	.	x	.	.	.	.	.	.	.	.	x	.	.
Simosthenurus sp. indet.	.	.	.	.	.	.	.	.	.	.	.	.	.	.	.	x	.	.	.	.	.	x	.	.	.	.	.	.	.	.
Sthenurus andersoni	.	cf.	.	.	.	cf.	.	.	.	x	.	.	.	.	.	.	.	.	x	.	**X**	.	.	.	.	.	.	.	.	.
Sthenurus atlas	.	.	.	.	.	.	.	.	.	x	.	.	.	.	.	.	.	.	.	.	.	.	.	.	.	.	.	.	.	.
Sthenurus stirlingi	.	.	.	.	.	.	.	.	.	.	.	.	.	.	.	.	.	.	.	.	**X**	.	.	.	.	.	.	.	.	.
Sthenurus tindalei	.	.	.	.	.	.	.	.	.	x	.	.	.	.	.	.	.	.	.	.	**X**	.	.	.	.	.	.	.	.	.
Sthenurus sp. indet.	.	.	.	.	.	.	x	.	x	.	.	.	.	.	x	.	.	.	.	.	.	.	.	.	.	.	.	.	.	.
Wallabia kitcheneri	.	.	.	.	.	.	.	.	.	.	.	.	.	.	.	.	.	.	.	.	.	.	.	x	.	.	.	x	.	.

*Site 6, units 5, 6a, and 6b. †Site 6, units 7 to 12.

whereas the sites in eastern Australia consist mainly of aeolian deposits along the edges of former or present lake basins, river or swamp deposits, and coastal dune deposits. To maximize our prospects of encountering fossils close in age to the terminal extinction event, we chose sites that geomorphological and stratigraphic evidence indicated were relatively young. The most recent megafaunal site may not be included in our survey, but we consider that a sufficient number of sites (n = 28) have been dated to discern a clear pattern in the distribution of burial ages.

A review (*15*) of 91 radiocarbon (^{14}C) ages obtained for Australian megafauna before 1995 rejected the vast majority of ages as being unreliable (*16*), including all those younger than 28 ka before the present (B.P.). The remaining ^{14}C ages were close to or beyond the practical limits of the technique, or were on materials that had ambiguous associations with the megafaunal remains. Radiocarbon dating of bone and charcoal older than 35 ka is problematic using conventional sample pretreatments (*17–19*). Consequently, ^{14}C ages were used in this study only for comparison with ages of <50 ka obtained

Table 2. Optical ages for burial sediments, supporting data, and sample contexts.

Site*	Sample context†	Grain size (μm)	Dose rate‡ (Gy ka^{-1})	Paleodose‡ (Gy)	Optical age‡ (ka)
Queensland					
1. Ned's Gully¶	Megafaunal unit, sample 1	180–212	0.76 ± 0.09	35 ± 2	47 ± 6
	Megafaunal unit, sample 2	90–125	0.78 ± 0.09	36 ± 3	46 ± 6
New South Wales					
2. Mooki River	Megafaunal unit	90–125	1.77 ± 0.16	74 ± 4	42 ± 4
3. Cox's Creek (Bando)¶	Megafaunal unit, sample 1	90–125	1.43 ± 0.14#	75 ± 3	53 ± 5
	Megafaunal unit, sample 1	180–212	1.38 ± 0.14#	75 ± 3	54 ± 6
	Megafaunal unit, sample 2	90–125	1.43 ± 0.14#	72 ± 6	50 ± 6
4. Cox's Creek (Kenloi)¶	5 cm above megafaunal unit	90–125	0.93 ± 0.06	47 ± 2	51 ± 4
	30 cm below megafaunal unit	90–125	0.97 ± 0.06	51 ± 2	53 ± 4
	30 cm below megafaunal unit	180–212	0.94 ± 0.06	54 ± 3	58 ± 4
5. Tambar Springs	Megafaunal unit (spit 4)	90–125	1.43 ± 0.09	2.9 ± 0.2	2.0 ± 0.2
6. Cuddie Springs	Above main megafaunal unit (unit 4)	90–125	2.47 ± 0.15	<41.3 ± 1.2	<16.7 ± 1.2
	Megafaunal unit (unit 5)	90–125	2.22 ± 0.14	<59 ± 2	<27 ± 2
	Megafaunal unit (unit 6a)	90–125	1.95 ± 0.12	<59 ± 3	<30 ± 2
	Megafaunal unit (unit 6b)	90–125	2.72 ± 0.17	<99 ± 5	<36 ± 3
7. Lake Menindee (Sunset Strip)¶	Megafaunal unit	180–212	1.69 ± 0.09	113 ± 8	67 ± 6
8. Willow Point¶	Attached to MV specimen	90–125	0.86 ± 0.08	47 ± 2	55 ± 6
9. Lake Victoria (site 50)¶	Attached to MV specimen	180–212	0.59 ± 0.07§	30 ± 3	52 ± 8
10. Lake Victoria (site 51)¶	Attached to MV specimen	90–125	0.71 ± 0.08	38 ± 2	54 ± 7
11. Lake Victoria (site 73)¶	Attached to MV specimen	90–125	1.71 ± 0.18	165 ± 5	97 ± 11
Victoria					
12. Montford's Beach¶	Attached to MV specimen	90–125	0.83 ± 0.10	>49.7 ± 1.2	>60 ± 7
13. Lake Weering¶	Attached to MV specimen	90–125	1.42 ± 0.15#	117 ± 3	82 ± 9
14. Lake Corangamite	Attached to MV specimen, sample 1	90–125	1.50 ± 0.18	79 ± 4	52 ± 7
	Attached to MV specimen, sample 1	180–212	1.47 ± 0.18	78 ± 4	53 ± 7
	Attached to MV specimen, sample 2	180–212	1.46 ± 0.17	70 ± 4	48 ± 6
15. Lake Weeranganuk¶	Attached to MV specimen	180–212	6.3 ± 0.7#	437 ± 18	70 ± 8
16. Lake Colongulac¶	Attached to MV specimen	180–212	1.59 ± 0.16§	131 ± 10	82 ± 10
17. Warrnambool¶	From MV sediment slab with footprint	180–212	0.61 ± 0.08	37 ± 3	60 ± 9
South Australia					
18. Victoria Fossil Cave (Grant Hall)	20 cm below top of megafaunal unit	90–125	1.28 ± 0.08	107 ± 9	84 ± 8
19. Victoria Fossil Cave (Fossil Chamber)¶	50 cm below top of megafaunal unit	90–125	0.67 ± 0.04	115 ± 6	171 ± 14
	50 cm below top of megafaunal unit	180–212	0.65 ± 0.04	102 ± 8	157 ± 16
20. Wood Point	Unit containing eggshell	90–125	1.60 ± 0.14#	88 ± 3	55 ± 5
21. Lake Callabonna¶	Attached to MV specimen	90–125	0.62 ± 0.07	46 ± 2	75 ± 9
Western Australia					
22. Devil's Lair	Above main megafaunal unit (layer 28)	90–125	1.22 ± 0.05	51 ± 2	42 ± 2
	Megafaunal unit (layer 32)	90–125	1.71 ± 0.07#	79 ± 3	47 ± 2
	Megafaunal unit (layer 39)	90–125	1.35 ± 0.06	65 ± 2	48 ± 3
23. Kudjal Yolgah Cave¶	Megafaunal unit (pit 2)	90–125	1.11 ± 0.05	51 ± 2	46 ± 2
	Attached to WAM specimen	125–250	1.22 ± 0.14	56 ± 2	46 ± 6
24. Mammoth Cave¶	Upper megafaunal unit	90–125	0.72 ± 0.09	40 ± 4	55 ± 9
	Attached to WAM specimen, sample 1	90–125	1.04 ± 0.15	66 ± 2	63 ± 9
	Attached to WAM specimen, sample 2	90–125	0.90 ± 0.12	67 ± 3	74 ± 10
25. Moondyne Cave¶	Megafaunal unit	90–125	0.68 ± 0.05#	89 ± 7	131 ± 14
26. Tight Entrance Cave	Megafaunal unit (unit J)	90–125	0.72 ± 0.04	24 ± 3	33 ± 4
	Megafaunal unit (unit H)	90–125	0.52 ± 0.03	23 ± 3	45 ± 6
	Megafaunal unit (unit D)	90–125	0.73 ± 0.04	103 ± 14	141 ± 21
27. Du Boulay Creek¶	Attached to WAM specimen	90–125	2.7 ± 0.3#	>215 ± 22	>80 ± 12
West Papua					
28. Kelangurr Cave	Megafaunal unit	90–125	1.07 ± 0.10§	17.6 ± 1.0	16 ± 2

*Sites with taxa represented by articulated remains are marked by ¶. †MV and WAM indicate sediment removed from megafaunal collections at the Museum of Victoria and Western Australian Museum, respectively. ‡Mean ± 1σ uncertainty. Samples with a significant deficit of ^{238}U compared to ^{226}Ra are marked by #, and those with a significant excess of ^{238}U over ^{226}Ra are marked by §. Paleodose values include ±2% uncertainty associated with laboratory beta-source calibration. The Cuddie Springs (site 6) samples have multiple paleodose populations, of which the highest are shown (*29*). The Montford's Beach (site 12) and Du Boulay Creek (site 27) samples have paleodose distributions consistent with partial bleaching (*37*), so the minimum paleodose values and age estimates [obtained using a minimum age model (*35*)] are shown. The high paleodose of the Lake Weeranganuk (site 15) sample was obtained from aliquots with saturating exponential plus linear growth curves of luminescence intensity versus dose (*36*). This sample also has an unusually high dose rate, which is due to concentrations of >20 ppm of all radionuclides in the ^{238}U decay series. If these concentrations were lower in the past, then the optical age would be older.

from optical dating of megafauna-bearing sediments and $^{230}Th/^{234}U$ dating of flowstones formed above and below megafaunal remains. Optical dating is a luminescence-based method that indicates the time elapsed since the sediment grains were last exposed to sunlight (*20–22*). The optical age corresponds to the burial age of megafaunal remains in primary deposition, whereas $^{230}Th/^{234}U$ dating gives the crystallization age of the flowstone, and thus a constraining age for remains above or below the flowstone. Support for the optical ages reported here (Table 2) is provided by their consistency with the ^{14}C and $^{230}Th/^{234}U$ ages obtained at megafaunal sites where comparisons have been made (Table 3) (*19, 23–25*). All three methods yield concordant ages within the time range of ^{14}C dating, and beyond this limit the optical and $^{230}Th/^{234}U$ ages are in good agreement and correct stratigraphic order.

Optical and $^{230}Th/^{234}U$ dating were conducted primarily on deposits containing the remains of megafauna in articulated anatomical position (Table 1) to avoid uncertainties introduced by post-depositional disturbance and reworking of fossils. This conservative approach is vital because the remains must be in primary depositional context to estimate the time of death from optical dating of the burial sediments or $^{230}Th/^{234}U$ dating of the enclosing flowstones. We also dated some deposits with disarticulated remains, but we recognize that these ages will be too young if the remains have been derived from older units. A sandstone slab bearing the impression of a *Genyornis* footprint and dune sands containing burnt fragments of *Genyornis* eggshell were also dated. Sediment samples for optical dating were collected on site from stratigraphic units that were clearly related to the megafaunal remains; in addition, lumps of sediment attached to megafaunal remains in museum collections were removed for dating (Table 2). We adopted a conservative approach to dating of museum samples (*20*), owing to their small size and the lack of an in situ dose rate measurement. Confidence in the age estimates for the museum specimens is given by the close agreement between the ages of the museum and field-collected samples from Kudjal Yolgah Cave (site 23; see Table 2). Our main conclusions, however, are based on field-collected samples, which yield the most reliable and precise ages. Calcite flowstones were prepared for $^{230}Th/^{234}U$ dating using standard methods and were analyzed by thermal ionization mass spectrometry (*19, 24, 25*), and the ages (Table 3) have been corrected for detrital ^{230}Th contamination (*26*).

The youngest optical ages obtained for deposits with articulated megafaunal remains (Table 2) (*27*) are 47 ± 4 ka for Ned's Gully (site 1) in Queensland and 46 ± 2 ka for Kudjal Yolgah Cave (site 23) in Western Australia. This result implies broadly synchronous extinction across the continent. Claims have also been made (*28*) for articulated remains of *Simosthenurus occidentalis* of similar age from Tight Entrance Cave (site 26, unit H or below) in Western Australia, and several sites (3, 4, 8, 9, and 10) in New South Wales produced slightly older ages (50 to 55 ka) for articulated megafauna. In contrast, much younger apparent burial ages were obtained for some sites containing disarticulated remains (Table 2) (*27*); the youngest such age is 2.0 ± 0.2 ka for fragmented remains at Tambar Springs (site 5). Optical dating of individual grains from the Cuddie Springs deposit [site 6 (*23*)] indicates that some sediment mixing has occurred (*29*). We interpret the young ages obtained for disarticulated remains and the indication of sediment mixing at Cuddie Springs as evidence that the remains are not in their primary depositional setting, but have been eroded from older units and redeposited in younger units with contemporaneous sediment and charcoal.

The youngest measured burial age for articulated remains may be older than the terminal extinction event, unless the most recent burial site is fortuitously included in our survey. But each optical age has a relative standard error of 5 to 15%, so the measured age could by chance be less than the true extinction age at some sites. Accordingly, we built a statistical model of the data under the assumption that the true burial ages are a realization of a Poisson process of constant intensity up to the time of extinction. That is, we assumed that the true burial ages are distributed randomly through time, with equal numbers per unit time, on average. The optical age is the true burial age plus a Gaussian error with a mean of zero and a standard deviation equal to the reported standard error. We estimated the time of extinction by maximum likelihood, confining attention to articulated remains with optical ages of ≤55 ka (*30*). This avoids a potential difficulty caused by the undersampling of sites much older than the extinction event. Using this model, the maximum likelihood estimate of the extinction time is 46.4 ka, with 68% and 95% confidence intervals of 48.9 to 43.6 ka and 51.2 to 39.8 ka, respectively.

Our data show little evidence for faunal attenuation. Twelve of the 20 genera of megafauna recorded from Pleistocene deposits in temperate Australia (*1, 2*) survived to at least 80 ka, including the most common and widespread taxa, and six of these genera (*Diprotodon*, *Phascolonus*, *Thylacoleo*, *Procoptodon*, *Protemnodon*, and *Simosthenurus*) are represented at the two sites dated to around 46 ka. These data indicate that a relatively diverse group of megafauna survived until close to the time of extinction. Further sites are needed to test this proposition and to identify the cause(s) of megafaunal extinction.

Table 3. $^{230}Th/^{234}U$ ages for Western Australian flowstones, supporting data, and sample contexts. The subscripts (*t*) and (0) denote the present and initial values of $\delta^{234}U$, respectively. All errors are 2σ. Ages for flowstones at Devil's Lair (site 22), Tight Entrance Cave (site 26), and Victoria Fossil Cave (Grant Hall, site 18, and Fossil Chamber, site 19) are reported elsewhere (*19, 24, 25, 28*).

Site*	Sample context	Detrital Th correction†	U (ppm)	$^{230}Th/^{238}U$ activity ratio	$\delta^{234}U_{(t)}$ (‰)	$\delta^{234}U_{(0)}$ (‰)	$^{230}Th/^{232}Th$ activity ratio	$^{230}Th/^{234}U$ age (ka)
23. Kudjal Yolgah Cave	Above megafaunal unit, sample 1	U	0.008	0.302 ± 0.006	102 ± 12	112 ± 14	13.9 ± 0.2	34.7 ± 0.9
		C		0.294 ± 0.008	102 ± 31	112 ± 34		33.6 ± 1.6
	Above megafaunal unit, sample 2	U	0.008	0.331 ± 0.003	105 ± 7	117 ± 7	5.37 ± 0.05	38.5 ± 0.6
		C		0.308 ± 0.005	105 ± 18	116 ± 19		35.4 ± 1.0
24. Mammoth Cave	Above upper megafaunal unit	U	0.025	0.375 ± 0.003	49 ± 3	57 ± 3	5.95 ± 0.05	47.9 ± 0.6
		C		0.353 ± 0.006	49 ± 16	56 ± 18		44.4 ± 1.3
	Below upper megafaunal unit	U	0.056	0.457 ± 0.005	73 ± 4	86 ± 5	4.49 ± 0.05	60.0 ± 1.0
		C		0.429 ± 0.009	72 ± 22	84 ± 25		55.2 ± 2.2
25. Moondyne Cave	Above megafaunal unit	U	0.061	0.341 ± 0.004	40 ± 4	45 ± 4	17.7 ± 0.3	43.1 ± 0.7
		C		0.335 ± 0.008	41 ± 24	46 ± 27		42.2 ± 1.8

*All three sites have taxa represented by articulated remains. †Data corrected (C) and uncorrected (U) for detrital ^{230}Th contamination (*26*). The detritally corrected ages are considered more reliable.

The burial ages for the last known megafaunal occurrence suggest that extinction occurred simultaneously in eastern and western Australia, and thus probably continent-wide, between 51 and 40 ka (95% confidence interval), at least 20 ka before the height of the Last Glacial Maximum. We estimate that the megafauna had vanished within 10 ± 5 ka of human arrival [56 ± 4 ka (*9–13*)] across a wide range of habitats and climatic zones. Megafaunal extinction in Australia occurred tens of millennia before similar events in North and South America, Madagascar, and New Zealand, each of which was preceded by the arrival of humans (*31*). A prediction of the "blitzkrieg" model of human-induced extinction [as proposed first for North America (*32*) and later for New Zealand (*33*)] is that megafaunal extinction should occur soon after human colonization, and that extinction is followed by widespread ecosystem disruption (*1*). Alternatively, human arrival may first have triggered ecosystem disruption, as a result of which the megafauna became extinct (*8*). The latter sequence of events allows for a substantial time interval between human colonization and megafaunal extinction, so that climatic factors may also be involved (*34*). There is sufficient uncertainty in the ages for both human colonization and megafaunal extinction that we cannot distinguish between these possibilities, but our data are consistent with a human role in extinction. Resolving this debate would require more precise ages for human colonization and megafaunal extinction, as well as an improved understanding of human interactions with the Australian landscape and biota during the earliest period of human occupation.

References and Notes

1. T. F. Flannery, *Archaeol. Oceania* **25**, 45 (1990).
2. P. Murray, in *Vertebrate Palaeontology of Australasia*, P. Vickers-Rich, J. M. Monaghan, R. F. Baird, T. H. Rich, Eds. (Pioneer Design Studio, Melbourne, 1991), pp. 1071–1164.
3. T. F. Flannery, R. G. Roberts, in *Extinctions in Near Time: Causes, Contexts, and Consequences*, R. D. E. MacPhee, Ed. (Kluwer Academic/Plenum, New York, 1999), pp. 239–255.
4. C. S. Wilkinson, *Proc. Linn. Soc. New South Wales* **9**, 1207 (1884).
5. R. Owen, *Researches on the Fossil Remains of the Extinct Mammals of Australia* (Erxleben, London, 1877).
6. D. Merrilees, *J. R. Soc. West. Austr.* **51**, 1 (1968).
7. R. Jones, *Archaeol. Phys. Anthropol. Oceania* **3**, 186 (1968).
8. G. H. Miller *et al.*, *Science* **283**, 205 (1999).
9. R. G. Roberts, R. Jones, M. A. Smith, *Nature* **345**, 153 (1990).
10. R. G. Roberts *et al.*, *Quat. Sci. Rev.* **13**, 575 (1994).
11. ———, *Ancient TL* **16**, 19 (1998).
12. J. M. Bowler, D. M. Price, *Archaeol. Oceania* **33**, 156 (1998).
13. A. Thorne *et al.*, *J. Hum. Evol.* **36**, 591 (1999).
14. D. R. Horton, in *Quaternary Extinctions: A Prehistoric Revolution*, P. S. Martin, R. G. Klein, Eds. (Univ. of Arizona Press, Tucson, AZ, 1984), pp. 639–680.
15. A. Baynes, *Rec. West. Austr. Mus.* (suppl. 57), 391 (1999).
16. D. J. Meltzer, J. I. Mead, in *Environments and Extinctions: Man in Late Glacial North America*, J. I. Mead, D. J. Meltzer, Eds. (Center for the Study of Early Man, Univ. of Maine, Orono, ME, 1985), pp. 145–173.
17. J. P. White, T. F. Flannery, *Austr. Archaeol.* **40**, 13 (1995).
18. S. Van Huet, R. Grün, C. V. Murray-Wallace, N. Redvers-Newton, J. P. White, *Austr. Archaeol.* **46**, 5 (1998).
19. C. S. M. Turney *et al.*, *Quat. Res.* **55**, 3 (2001).
20. Optical ages were calculated from the burial dose (paleodose), measured using the photon-stimulated luminescence (PSL) signal, divided by the dose rate due to ionizing radiation (*21, 22*). The portion of each sample exposed to daylight was first removed under dim red illumination and discarded. Quartz grains in three ranges of diameter (90 to 125 μm, 180 to 212 μm, and 125 to 250 μm) were extracted from the remaining sample using standard procedures (*22*) and etched in 40% hydrofluoric acid for 45 min. As a test of internal consistency, some stratigraphic units were dated using more than one sample or grain-size fraction. Paleodoses were obtained using single-aliquot regenerative-dose protocols, statistical models, and experimental apparatus as described (*35–37*). Each aliquot was illuminated for 100 to 125 s at 125°C, and paleodoses were calculated from the first 3 to 5 s of PSL arising from the burial, regenerative, and test doses, using the final 20 s as background. Each sample was given a preheat plateau test (*22*) using aliquots composed of >100 grains, and a repeat regenerative dose was given to verify that the protocol yielded the correct (known) dose (*35, 36*). The paleodoses in Table 2 were obtained from aliquots typically composed of <10 grains to permit detection of insufficient bleaching before burial from examination of the paleodose distribution (*37*). For samples with clearly asymmetrical (positively skewed) distributions, mean paleodoses were calculated using the minimum age model (*35*); the central age model (*35*) was used for other samples. For some samples, paleodoses were also obtained using the standard multiple-aliquot additive-dose method (*22*). The dose rates due to ^{238}U and ^{232}Th (and their daughter products) and due to ^{40}K were calculated from a combination of high-resolution gamma and alpha spectrometry (to check for disequilibria in the ^{238}U and ^{232}Th decay series), thick-source alpha counting, x-ray fluorescence of powdered samples, and field measurements of the gamma dose rate. Cosmic-ray dose rates were estimated from published data [J. R. Prescott, J. T. Hutton, *Radiat. Meas.* **23**, 497 (1994)] and an effective internal alpha dose rate of 0.03 Gy ka^{-1} was assumed for all samples. Gamma and beta dose rates were corrected for the estimated long-term water content of each sample and for beta-dose attenuation [V. Mejdahl, *Archaeometry* **21**, 61 (1979)]. We used the sediment farthest from the bone to date the museum specimens to minimize any dose rate heterogeneity in the sediments adjacent to the bone. The gamma dose rates for the museum specimens were estimated from the attached lumps of sediment and from sediment-bone mixtures, using an uncertainty of ±20% to accommodate any spatial inhomogeneity in the gamma radiation field. This uncertainty was also applied to field samples collected without measuring the in situ gamma dose rate; in situ measurements had uncertainties of less than ±5%. Some samples had a significant deficit or excess of ^{238}U with respect to ^{226}Ra (see Table 2). The optical ages for these samples were calculated using the measured radionuclide concentrations, but any error due to post-burial uranium migration should be accommodated within the age uncertainties.
21. D. J. Huntley, D. I. Godfrey-Smith, M. L. W. Thewalt, *Nature* **313**, 105 (1985).
22. M. J. Aitken, *An Introduction to Optical Dating: The Dating of Quaternary Sediments by the Use of Photon-Stimulated Luminescence* (Oxford Univ. Press, Oxford, 1998).
23. J. Field, J. Dodson, *Proc. Prehist. Soc.* **65**, 275 (1999).
24. L. K. Ayliffe *et al.*, *Geology* **26**, 147 (1998).
25. K. C. Moriarty, M. T. McCulloch, R. T. Wells, M. C. McDowell, *Palaeogeogr. Palaeoclimatol. Palaeoecol.* **159**, 113 (2000).
26. Ages corrected for detrital ^{230}Th contamination were obtained by determining the thorium and uranium isotope compositions for different splits of the same flowstone (each split containing different proportions of the detrital end member and the pure authigenic calcite phase). Mixing line plots of $^{230}Th/^{232}Th$ versus $^{238}U/^{232}Th$, and of $^{234}U/^{232}Th$ versus $^{238}U/^{232}Th$, provide estimates of the detritally corrected $^{230}Th/^{238}U$ and $^{234}U/^{238}U$ ratios as well as the isotope ratios of the detrital end member phases: $^{230}Th/^{232}Th = 0.37 \pm 0.04$, $^{234}U/^{232}Th = 0.00 \pm 0.03$ (Kudjal Yolgah Cave); $^{230}Th/^{232}Th = 0.36 \pm 0.02$, $^{234}U/^{232}Th = 0.00 \pm 0.02$ (Mammoth Cave, upper flowstone); $^{230}Th/^{232}Th = 0.28 \pm 0.03$, $^{234}U/^{232}Th = 0.01 \pm 0.03$ (Mammoth Cave, lower flowstone); and $^{230}Th/^{232}Th = 0.29 \pm 0.04$, $^{234}U/^{232}Th = 0.00 \pm 0.01$ (Moondyne Cave, using the average detrital end member isotope ratios from five nearby sites). The half-lives of ^{234}U and ^{230}Th used in the age calculation are 244,600 ± 490 years and 75,381 ± 590 years, respectively.
27. See the supplementary figure at *Science* Online (www.sciencemag.org/cgi/content/full/292/5521/1888/DC1).
28. G. J. Prideaux, G. A. Gully, L. K. Ayliffe, M. I. Bird, R. G. Roberts, *J. Vertebr. Paleontol.* **20** (suppl. to no. 3), 62A (2000).
29. Single-grain optical dating and finite mixture models [R. G. Roberts, R. F. Galbraith, H. Yoshida, G. M. Laslett, J. M. Olley, *Radiat. Meas.* **32**, 459 (2000)] were used to distinguish paleodose (and hence age) populations in the sediment samples. Multiple discrete populations were identified, which we attribute to the mixing of grains with different burial histories. The populations with the highest paleodoses (Table 2) yielded optical ages consistent with the ^{14}C ages obtained from pieces of charcoal (*23*).
30. We cannot be certain that articulated remains were recovered from the upper megafaunal unit at Mammoth Cave (site 24), so the optical age of 55 ± 9 ka was not included in the data set.
31. P. S. Martin, D. W. Steadman, in *Extinctions in Near Time: Causes, Contexts, and Consequences*, R. D. E. MacPhee, Ed. (Kluwer Academic/Plenum, New York, 1999), pp. 17–55.
32. P. S. Martin, *Science* **179**, 969 (1973).
33. R. N. Holdaway, C. Jacomb, *Science* **287**, 2250 (2000).
34. Much of the 60- to 40-ka interval was marked by generally wetter conditions than at present in both eastern Australia (*24, 38*) [G. C. Nanson, D. M. Price, S. A. Short, *Geology* **20**, 791 (1992); J. M. Bowler, *Archaeol. Oceania* **33**, 120 (1998)] and southwestern Australia [J. Balme, D. Merrilees, J. K. Porter, *J. R. Soc. West. Austr.* **61**, 33 (1978), using the revised chronology for Devil's Lair (*19*)]. But monsoonal activity may have been variable with short-lived climatic oscillations (*38*), in keeping with evidence from deep-sea cores of climate instability [J. P. Sachs, S. J. Lehman, *Science* **286**, 756 (1999); S. L. Kanfoush *et al.*, *Science* **288**, 1815 (2000)].
35. R. F. Galbraith, R. G. Roberts, G. M. Laslett, H. Yoshida, J. M. Olley, *Archaeometry* **41**, 339 (1999).
36. H. Yoshida, R. G. Roberts, J. M. Olley, G. M. Laslett, R. F. Galbraith, *Radiat. Meas.* **32**, 439 (2000).
37. J. M. Olley, G. G. Caitcheon, R. G. Roberts, *Radiat. Meas.* **30**, 207 (1999).
38. B. J. Johnson *et al.*, *Science* **284**, 1150 (1999).

39. We thank S. Eberhard, J. Field, G. Gully, L. Hatcher, R. McBeath, D. Merrilees, G. Miller, R. Molnar, K. Moriarty, A. Ritchie, I. Sobbe, the late G. van Tets, J. Wilkinson, D. Witter, T. Worthy, and R. Wright for sample collection, field assistance, and discussions; the Western Australian Museum and Museum of Victoria for permission to access their collections; M. Olley for preparing the gamma spectrometry samples; R. Galbraith for mixture modeling; and R. Gillespie and O. Lian for comments. Supported by a Large Grant and a Queen Elizabeth II Fellowship from the Australian Research Council (R.G.R.).

27 February 2001; accepted 25 April 2001